



# New soliton molecules to couple of nonlinear models: ion sound and Langmuir waves systems

Syed T. R. Rizvi<sup>1</sup> · Aly R. Seadawy<sup>2</sup> · S. Oan Abbas<sup>1</sup> · Komal Naz<sup>1</sup>

Received: 1 October 2022 / Accepted: 5 October 2022 / Published online: 22 October 2022  
© The Author(s), under exclusive licence to Springer Science+Business Media, LLC, part of Springer Nature 2022

## Abstract

In this paper, we will study two various nonlinear models: the Atangana–Baleanu fractional system of equations for the ion sound and Langmuir waves (ISALWs) and Hirota Ramani equation to obtain variety of solitary wave solutions. We will obtain bright, dark, periodic wave and solitony wave for ISALWs equation. We will also retrieved bell type, kink type, singular, Jacobion elliptic function, Weierstrass-elliptic function, hyperbolic functions, periodic functions and other solitary wave solutions for Hirota Ramani equation using Sub ODE technique under some constraint conditions. At the end we will present our solutions with the help of graphs in distinct dimensions.

**Keywords** Integrability · Solitons · Fractional calculus

## 1 Introduction

Recently, the number of applications of fractional calculus is growing speedily. Fractional differential equations (FDEs) are used in various areas of nonlinear sciences like diffusion, electrical circuits, economy, control problem, etc. (Sheng et al. 2020). Nonlinear FDE (NLFDE) have gained high attention and interest for researchers. These equations possess huge network of applications in the subject of physics and engineering fields with the development of corresponding theories. In real life, the solution of these types of equations have significant effects in the form of traveling waves. The theory of fractional derivatives (FD) is also helpful in physiology, medical science, and epidemic diseases (Rezazadeh et al. 2021; Younas et al. 2021; Akram et al. 2021; Seadawy et al. 2021c, 2021d, 2021e; Bilal et al. 2021; Rizvi et al. 2021b, c; Seadawy et al. 2021a; Tariq et al. 2021; Ahmad et al. 2021; Bashir et al. 2021; Seadawy et al. 2021b). There are so many types of FDs like Reimann Liouville, Caputo-Fabrizio and the Atangana Baleanu fractional derivatives (ABFD) (Syama and Al-Refai 2019; Atangana 2018). Mittag Leffler function is used in

---

✉ Aly R. Seadawy  
aabelalim@taibahu.edu.sa

<sup>1</sup> Department of Mathematics, COMSATS University Islamabad, Lahore Campus, Islamabad, Pakistan

<sup>2</sup> Mathematics Department, Faculty of Science, Taibah University, Al-Madinah Al-Munawarah 41411, Kingdom of Saudi Arabia

ABFD as non local and non singular kernels accepting all properties of FD. Antangana and Koca (2016) used ABFD in nonlinear system and discussed the uniqueness and existence of the fractional order system. In the field of fractional calculus, ABFD is used to sort out many problems (Antangana and Baleanu 2016; Fernandez et al. 2019; Baleanu et al. 2018; Bas and Ozarslan 2018). Ghanbari and Antangana (2020) studied some applications of ABFD in image processing. Jarad et al. (2018) studied uniqueness and existence conditions for numerous ordinary differential equations with ABFD. Owolabi (2018) displayed relationship between dynamical system and ABFD. Peter et al. (2021) used AB Operator to analyse fractional order mathematical model of COVID-19 in Nigeria. Recently, many integration architectonics such as new extended auxiliary scheme (Rizvi et al. 2020a),  $\frac{G'}{G}$ -expansion method (Abazari 2016), csch method, extended tanh-coth mechanism and extended rational sinh-cosh process (Rizvi et al. 2020b), generalized exponential rational function method (Ghanbari et al. 2019), Jacobi elliptic function expansion scheme (Kurt 2019), sub-ode method (Zayeda et al. 2019) and many other have been used to find exact solutions for different nonlinear evolution and FDEs(Ahmed et al. 2019b, Dianchen 2018, Khater et al. 2006, Seadawy et al. 2019b, c). Our aim is to obtain some new types of solitary waves for ISALWs with ABFD and Hirota Ramani model with the aid of sub ode scheme.

The ISLAWs with ABFD is given by Rezazadeh et al. (2021)

$${}_t^{ABR}D_{0^+}^\alpha J + \frac{1\partial^2 J}{2\partial x^2} - rJ = 0,$$

$$t > 0, 0 < \alpha \leq 1$$

$${}_t^{ABR}D_{0^+}^\alpha r - \frac{\partial^2 r}{\partial x^2} - 2\frac{\partial^2(|J|^2)}{\partial x^2} = 0, \tag{1}$$

here normalised density, electric field and AB fractional operator are represented by  $r$ ,  $Je^{-i\omega_p t}$  and  ${}_t^{ABR}D_{0^+}^\alpha$  respectively.

$${}_t^{ABR}D_{a^+}^\alpha g(t) = \frac{\varpi(\alpha)}{1-\alpha} \frac{d}{dt} \int_a^t g(x)\Omega_\alpha\left(\frac{-\alpha(t-\alpha)^\alpha}{1-\alpha}\right) dx, \tag{2}$$

where  $\Omega_\alpha(\cdot)$  is Mittag–Leffler function, which is given as

$$\Omega_\alpha\left(\frac{-\alpha(t-\alpha)^\alpha}{1-\alpha}\right) = \sum_{r=0}^\infty \frac{\left(\frac{-\alpha}{1-\alpha}\right)^q (t-x)^{\alpha q}}{\Gamma(\alpha q + 1)},$$

normalization function defined by  $\varpi(\alpha)$ . Thus, we get the AB fractional operator

$${}_t^{ABR}D_{a^+}^\alpha g(t) = \frac{\varpi(\alpha)}{1-\alpha} \sum_{q=0}^\infty \left(\frac{-\alpha}{1-\alpha}\right)^q RLI_a^{\alpha q} g(t)$$

The second model is known as Hirota Ramani equations given by Roshid and Alam (2017)

$$\Theta_t - \Theta_{xxt} + A\Theta_x(1 - \Theta_t) = 0, \tag{3}$$

where  $\Theta = \Theta(x, t)$  is the amplitude of the wave mode and  $A \neq 0$  is a real constant.

The paper is arranged as follows: in Sect. 2, we will describe sub ode scheme, in Sect. 3, we will apply our tehniqe to ISLAWs with ABFD, in Sect. 4, we will find solitary wave

solutions for Hirota Ramani equation with our scheme. In Sect. 5, we will discuss our results and at the end in Sect. 6, we will provide conclusion.

## 2 Sub-ODE method

To approach this sub ode, we suppose the following solution: (Rizvi et al. 2020c, 2021a)

$$G(\eta) = \mu M^m(\eta), \quad \mu > 0 \tag{4}$$

here  $m$  is a parameter and  $M(\eta)$  satisfies the equation:

$$M'^2(\eta) = \Upsilon M^{2-2p}(\eta) + \Delta M^{2-p}(\eta) + \Lambda M^2(\eta) + \Pi M^{2+p}(\eta) + \Psi M^{2+2p}(\eta), \quad p > 0, \tag{5}$$

here  $\Upsilon, \Delta, \Lambda, \Pi$  and  $\Psi$  are constants. By using homogeneous balance method we can find  $m$  in (4) given as ,

$$D(\phi_1) = m, \quad D(\phi^2) = 2m, \dots \quad D(\phi') = m + p, \quad D(\phi'') = m + 2p, \dots \tag{6}$$

Thus Eq. (5) has following solutions cases:

**Case 1** When  $\Upsilon = \Delta = \Pi = 0$ , we have a bell type soliton solution for Eq. (5) as:

$$G(\eta) = \left[ \sqrt{-\frac{\Lambda}{\Psi}} \sec h(\sqrt{\Lambda p \eta}) \right]^{\frac{1}{p}}, \quad \Lambda > 0, \quad \Psi < 0, \tag{7}$$

a periodic solution

$$G(\eta) = \left[ \sqrt{-\frac{\Lambda}{\Psi}} \sec(\sqrt{-\Lambda p \eta}) \right]^{\frac{1}{p}}, \quad \Lambda < 0, \quad \Psi > 0, \tag{8}$$

and a rational solution

$$G(\eta) = \left[ \frac{\varepsilon}{\sqrt{\Psi p \eta}} \right]^{\frac{1}{p}}, \quad \Lambda = 0, \quad \Psi > 0, \quad \varepsilon = \pm 1. \tag{9}$$

**Case 2** If  $\Delta = \Pi = 0, \Upsilon = \frac{\Lambda^2}{4\Psi}$ , then Eq. (5) has a kink type soliton:

$$G(\eta) = \left[ \varepsilon \sqrt{-\frac{\Lambda}{\Psi}} \tanh(\sqrt{\Lambda p \eta}) \right]^{\frac{1}{p}}, \quad \Lambda > 0, \quad \Psi < 0, \quad \varepsilon = \pm 1, \tag{10}$$

and a periodic solution

$$G(\eta) = \left[ \varepsilon \sqrt{-\frac{\Lambda}{\Psi}} \tan(\sqrt{-\Lambda p \eta}) \right]^{\frac{1}{p}}, \quad \Lambda < 0, \quad \Psi > 0, \quad \varepsilon = \pm 1, \tag{11}$$

**Case 3** If  $\Delta = \Pi = 0$ , then Eq. (5) has following three Jacobian elliptic function (JEF) solutions:

$$G(\eta) = \left[ \sqrt{-\frac{\Lambda m^2}{\Psi(2m^2 - 1)}} \operatorname{cn} \left( \sqrt{\frac{\Lambda}{(2m^2 - 1)}} p\eta \right) \right]^{\frac{1}{p}}, \quad \Lambda > 0, \quad \Upsilon = \frac{\Lambda^2 m^2 (m^2 - 1)}{\Psi(2m^2 - 1)^2}, \tag{12}$$

$$G(\eta) = \left[ \sqrt{-\frac{\Lambda}{\Psi(2 - m^2)}} \operatorname{dn} \left( \sqrt{\frac{\Lambda}{(2 - m^2)}} p\eta \right) \right]^{\frac{1}{p}}, \quad \Lambda > 0, \quad \Upsilon = \frac{\Lambda^2 (1 - m^2)}{\Psi(2 - m^2)^2}, \tag{13}$$

and

$$G(\eta) = \left[ \sqrt{-\frac{\Lambda m^2}{\Psi(m^2 + 1)}} \operatorname{sn} \left( \sqrt{-\frac{\Lambda}{(m^2 + 1)}} p\eta \right) \right]^{\frac{1}{p}}, \quad \Lambda < 0, \quad \Upsilon = \frac{\Lambda^2 m^2}{\Psi(m^2 + 1)^2}. \tag{14}$$

**Case 6** For  $\Delta = \Pi = 0$ , the Weierstrass-elliptic function (WEF) solutions are obtained for Eq. (5) as:

$$G(\eta) = \left[ \frac{1}{\Psi} \wp(p\eta, g_2, g_3) - \frac{\Lambda}{3} \right]^{\frac{1}{2p}}, \tag{15}$$

where  $g_2 = \frac{4\Lambda^2}{3}$  and  $g_3 = \frac{4\Lambda(-2\Lambda^2)}{27}$ .

$$G(\eta) = \frac{3\sqrt{\Psi-1}\wp'(p\eta, g_2, g_3)^{\frac{1}{p}}}{6\wp(p\eta, g_2, g_3) + \Lambda}, \tag{16}$$

where  $g_2 = \frac{\Lambda^2}{12}$  and  $g_3 = 0$ .

**Case 7** If  $\Delta = \Pi = 0$  and  $\Upsilon = \frac{5\Lambda^2}{36\Psi}$  the Eq. (5) has following WEF solutions :

$$G(\eta) = \left[ \frac{\Lambda\sqrt{-\frac{15\Lambda}{2\Psi}}\wp(p\eta, g_2, g_3)}{3\wp(p\eta, g_2, g_3) + \Lambda} \right]^{\frac{1}{p}}, \tag{17}$$

where  $g_2 = \frac{2\Lambda^2}{9}$  and  $g_3 = \frac{\Lambda^3}{54}$ . Here  $g_2$  and  $g_3$  are known as invariant WEF.

**Case 8** For  $\Upsilon = \Delta = 0$ , the following bell type and kink type solutions for Eq. (5) are obtained:

$$G(\eta) = \left( \frac{1}{\cosh(\sqrt{\Lambda}p\eta)} \right)^{\frac{1}{p}}, \quad \Lambda > 0, \quad \Pi = 0, \quad \Psi = \frac{\Pi^2}{4\Lambda} - \Lambda, \tag{18}$$

$$G(\eta) = \left( \frac{1}{2} \sqrt{\frac{\Lambda}{\Psi}} \left[ 1 + \varepsilon \tanh \left( \frac{1}{2} \sqrt{\Lambda}p\eta \right) \right] \right)^{\frac{1}{p}}, \quad \Lambda > 0, \quad \Psi > 0, \quad \Pi = 0, \quad \varepsilon = \pm 1, \tag{19}$$

and

$$G(\eta) = \left( \frac{1}{(\frac{1}{2}p\eta)^2 - \Psi} \right)^{\frac{1}{p}}, \quad \Lambda = 0, \quad \Pi = 0, \quad \Psi = < 0. \tag{20}$$

**Case 9** For  $\Upsilon = \Delta = 0, \Lambda > 0$ , then the following hyperbolic functions solutions for Eq. (5) are obtained:

$$G(\eta) = \left[ \frac{2\Lambda \operatorname{sech}^2\left(\frac{\sqrt{\Lambda}}{2}p\eta\right)}{[\sqrt{-4\Lambda\Psi}] \operatorname{sech}^2\left(\frac{\sqrt{\Lambda}}{2}p\eta\right) - 2\sqrt{-4\Lambda\Psi}} \right]^{\frac{1}{p}}, \quad \Pi^2 - 4\Lambda\Psi > 0 \tag{21}$$

$$G(\eta) = \left( \frac{2\Lambda \operatorname{csch}^2\left(\frac{\sqrt{\Lambda}}{2}p\eta\right)}{[\sqrt{-4\Lambda\Psi}] \operatorname{csch}^2\left(\frac{\sqrt{\Lambda}}{2}p\eta\right) + 2\sqrt{-4\Lambda\Psi}} \right)^{\frac{1}{p}}, \quad \Pi^2 - 4\Lambda\Psi > 0 \tag{22}$$

**Case 10** For  $\Upsilon = \Delta = 0, \Lambda < 0$ , then the following periodic functions solutions for Eq. (5) are obtained:

$$G(\eta) = \left( \frac{2\Lambda \operatorname{sec}^2\left(\frac{\sqrt{-\Lambda}}{2}p\eta\right)}{[\sqrt{-4\Lambda\Psi}] \operatorname{sec}^2\left(\frac{\sqrt{-\Lambda}}{2}p\eta\right) - 2\sqrt{-4\Lambda\Psi}} \right)^{\frac{1}{p}}, \quad \Pi^2 - 4\Lambda\Psi > 0 \tag{23}$$

$$G(\eta) = \left( \frac{2\Lambda \operatorname{csc}^2\left(\frac{\sqrt{-\Lambda}}{2}p\eta\right)}{[\sqrt{-4\Lambda\Psi}] \operatorname{csc}^2\left(\frac{\sqrt{-\Lambda}}{2}p\eta\right) - 2\sqrt{-4\Lambda\Psi}} \right)^{\frac{1}{p}}, \quad \Pi^2 - 4\Lambda\Psi > 0 \tag{24}$$

### 3 Solitary wave solutions for Eq. (1)

We use the following transformation for Eq. (1),

$$J(x, t) = u(\eta)e^{i\mu}, \quad n(x, t) = v(\eta),$$

$$\mu = kx + \frac{\omega(1 - \alpha)t^{-q}}{B(\alpha)\sum_{q=0}^{\infty} \left(-\frac{\alpha}{1-\alpha}\right)^q \Gamma(1 - \alpha q)}, \quad \eta = \gamma x + \frac{\beta(1 - \alpha)t^{-q}}{B(\alpha)\sum_{q=0}^{\infty} \left(-\frac{\alpha}{1-\alpha}\right)^q \Gamma(1 - \alpha q)}, \tag{25}$$

here  $\beta$  and  $\omega$  are constants. By putting Eq. (25) into Eq. (1) we obtain

$$\frac{1}{2}\gamma^2 u'' + i(\beta + k\gamma)u' - 0.5(k^2 + 2\omega)u - uv = 0, \tag{26}$$

$$(\beta^2 - \gamma^2)v'' + 4\gamma^2(u'^2 - uu'') = 0, \tag{27}$$

Separating real and imaginary parts we get

$$\beta = -k\gamma \tag{28}$$

By double integration Eq. (27) we have

$$v = \frac{2\gamma^2}{\beta^2 - \gamma^2}u^2 = \frac{2}{k^2 - 1}u^2. \tag{29}$$

substituting Eqs. (28) and (29) into Eq. (26) provide us

$$u'' - \frac{4}{\gamma^2(k^2 - 1)}u^3 - \frac{(k^2 + 2w)}{\gamma^2}u = 0 \tag{30}$$

By homogeneous balancing method we get  $p = m$ .

$$u(\eta) = \mu G^p(\eta), \quad \mu > 0 \tag{31}$$

By putting Eq. (30) into Eq. (5), we get the following set of algebraic equations:

$$G^{3p}(\eta) : 2p^2\Psi\mu - \frac{4\mu^2}{(-1 + k^2)\gamma^2} = 0, \tag{32}$$

$$G^p(\eta) : \Lambda p^2\mu - \frac{k^2\mu}{\gamma^2} - \frac{2\mu\omega}{\gamma^2} = 0, \tag{33}$$

we have the following types of solutions:

**Type 1a** By substituting  $\Upsilon = \Delta = \Pi = 0$  in Eq. (5) and we get values of following parameters (Fig. 1).

$$\mu = \sqrt{\frac{\gamma^2 p^2 \Psi (k^2 - 1)}{2}}; \quad \Lambda = \frac{k^2 + w}{\gamma^2 p^2},$$

provided that

$$J_{1,1}(x, t) = \frac{\sqrt{(-1 + k^2)(-k^2 - 2w)} \operatorname{sech} \left( \eta \sqrt{k^2 + 2w} \right)}{\gamma \sqrt{2}}. \tag{34}$$

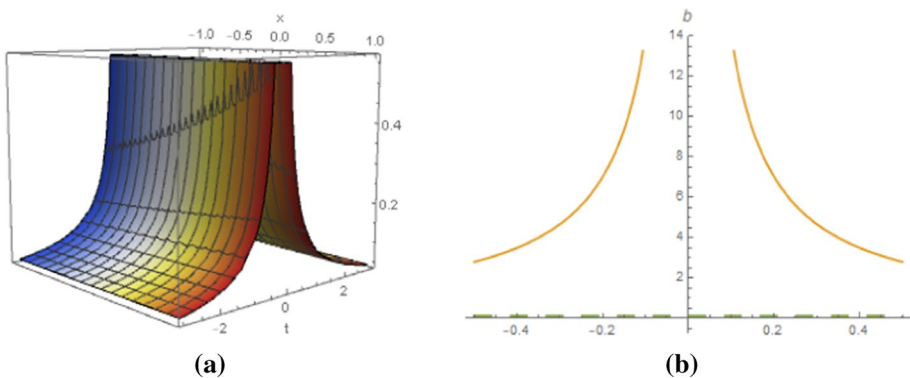


**Fig. 1** The dynamical behavior of the solution  $J_{1,1}(x, t)$  given by Eq. (34) is shown at  $p = 1, T = 5, \gamma = 20, K = 0.7, \omega = 7, r = 15, \alpha = -1, \beta = 3$

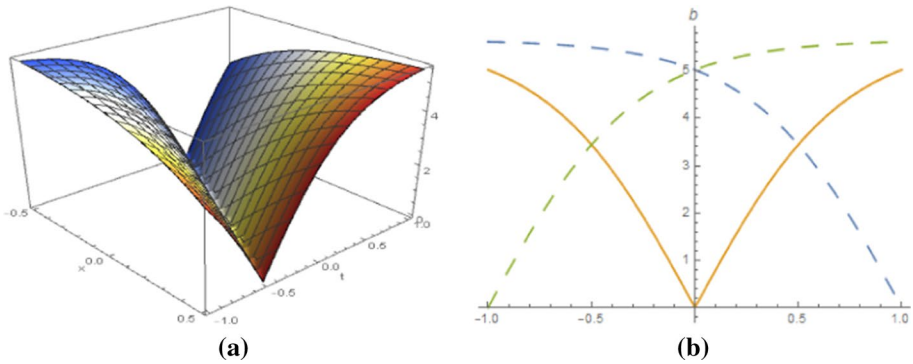


**Fig. 2** The dynamical behavior of the solution  $J_{1,2}(x, t)$  given by Eq. (29) is shown at  $p = 1, T = 5, \gamma = 0.1, K = 0.8, \omega = 0.6, r = 0.1, \alpha = 0.3, \beta = 0.7, \epsilon = 1$

**Type 1b** By substituting  $\Upsilon = \Delta = \Pi = 0$  in Eq. (5) and we get values of following parameters (Fig. 2).

$$\mu = \sqrt{\frac{\gamma^2 p^2 \Psi(k^2 - 1)}{2}}; \quad \Lambda = \frac{k^2 + w}{\gamma^2 p^2},$$

$$J_{1,2}(x, t) = \frac{\sqrt{(-1 + k^2)(-k^2 - 2w)} \tanh\left(\eta \sqrt{k^2 + 2w}\right) \epsilon}{\gamma \sqrt{2}}. \tag{35}$$

**Type 1c** By substituting  $\Upsilon = \Delta = \Pi = 0$  in Eq. (5) and we get values of following parameters and we obtained the solitary wave solutions (Fig. 3).

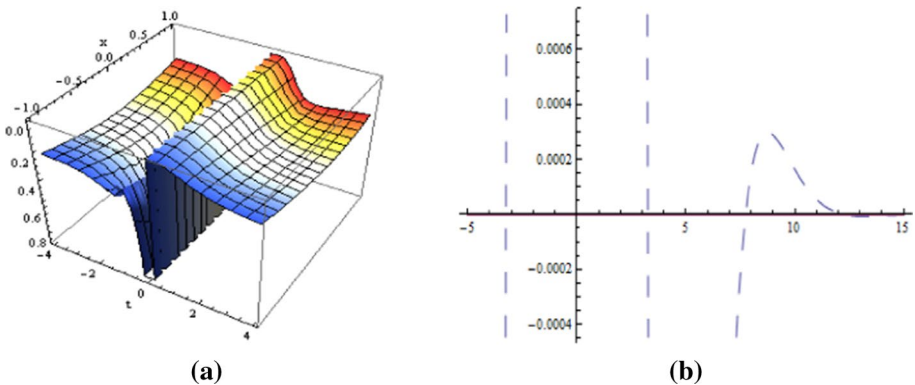


**Fig. 3** The dynamical behavior of the solution  $J_{1,3}(x, t)$  given by Eq. (30) is shown at  $p = 1, T = 5, \gamma = 0.1, K = 0.8, \omega = 0.6, r = 0.1, \alpha = 0.3, \beta = 0.7, \epsilon = 1$

$$\begin{aligned} \mu &= \sqrt{\frac{\gamma^2 p^2 \Psi(k^2 - 1)}{2}}; \quad \Lambda = \frac{k^2 + w}{\gamma^2 p^2}, \\ J_{1,3}(x, t) &= \frac{\sqrt{-1 + k^2} \gamma \epsilon}{\sqrt{2} \eta}. \end{aligned} \tag{36}$$

**Type 2a** By substituting  $\Upsilon = \Delta = \Pi = 0$  in Eq. (5) and we get values of following parameters and we obtain the kink and anti-kink type soliton solutions (Fig. 4).

$$\begin{aligned} \mu &= \sqrt{\frac{\gamma^2 p^2 \Psi(k^2 - 1)}{2}}; \quad \Lambda = \frac{k^2 + w}{\gamma^2 p^2}, \\ J_{2,1}(x, t) &= \frac{\sqrt{(-1 + k^2)(-k^2 - 2w)} \tanh\left(\eta \sqrt{k^2 + 2w}\right) \epsilon}{\gamma \sqrt{2}}. \end{aligned} \tag{37}$$

**Type 2b** By substituting  $\Upsilon = \Delta = \Pi = 0$  in Eq. (5) and we get values of following parameters and we obtain the kink and anti-kink type soliton solutions (Fig. 5).

$$\begin{aligned} \mu &= \sqrt{\frac{\gamma^2 p^2 \Psi(k^2 - 1)}{2}}; \quad \Lambda = \frac{k^2 + w}{\gamma^2 p^2}, \\ J_{2,2}(x, t) &= \frac{\sqrt{(-1 + k^2)(-k^2 - 2w)} \tanh\left(\eta \sqrt{-k^2 - 2w}\right) \epsilon}{\gamma \sqrt{2}}. \end{aligned} \tag{38}$$

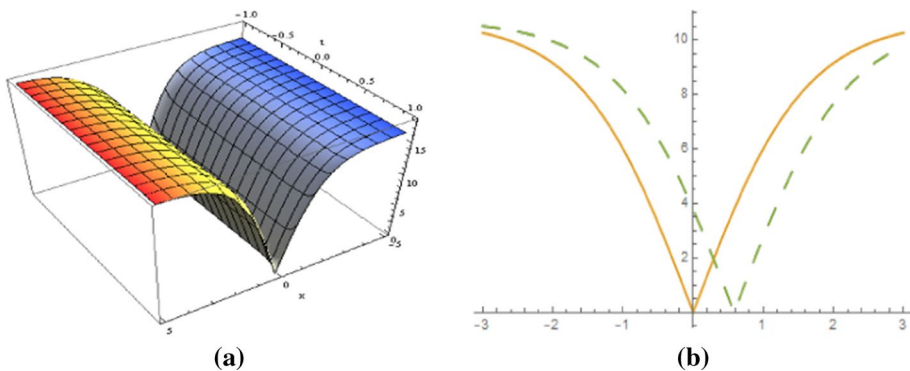


**Fig. 4** The dynamical behavior of the solution  $J_{2,1}(x, t)$  given by Eq. (31) at  $p = 1, T = 5, \gamma = 20, K = 0.7, \omega = 7, r = 10, \alpha = -1, \beta = 3, \epsilon = 1$



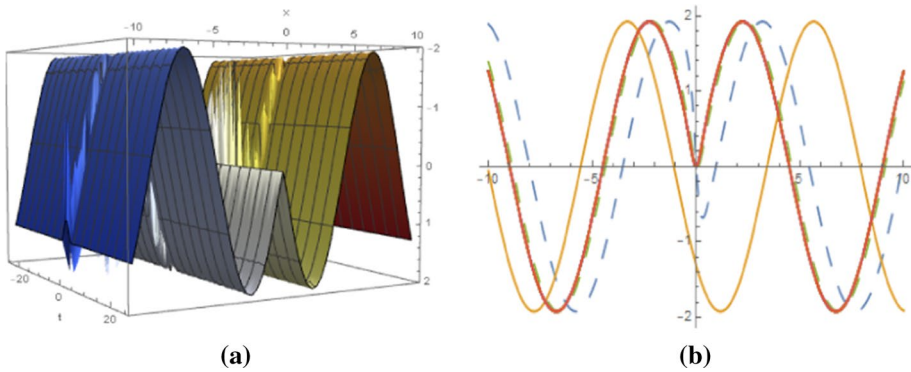


**Fig. 5** The dynamical behavior of the solution  $J_{2,2}(x, t)$  given by Eq. (32) is shown at  $p = 1, T = 5, \gamma = 20, K = 0.7, \omega = 7, r = 10, \alpha = -1, \beta = 3, \epsilon = 1$

**Type 3a**  $m \rightarrow 1$  By substituting  $\Delta = \Pi = 0$  in Eq. (5) and we get values of following parameters and we obtain the solitary wave solutions (Fig. 6).

$$\mu = \sqrt{\frac{\gamma^2 p^2 \Psi(k^2 - 1)}{2}}; \quad \Lambda = \frac{k^2 + w}{\gamma^2 p^2},$$

provided that

$$J_{3,1}(x, t) = \frac{\sqrt{(-1 + k^2)(-k^2 - 2w)} \operatorname{sech}\left(\eta \sqrt{\frac{k^2 + 2w}{\gamma}}\right)}{\sqrt{2}}. \tag{39}$$

**Type 3b**  $m \rightarrow 1$  By substituting  $\Delta = \Pi = 0$  in Eq. (5) and we get values of following parameters and we obtain the bell type soliton solutions (Fig. 7).

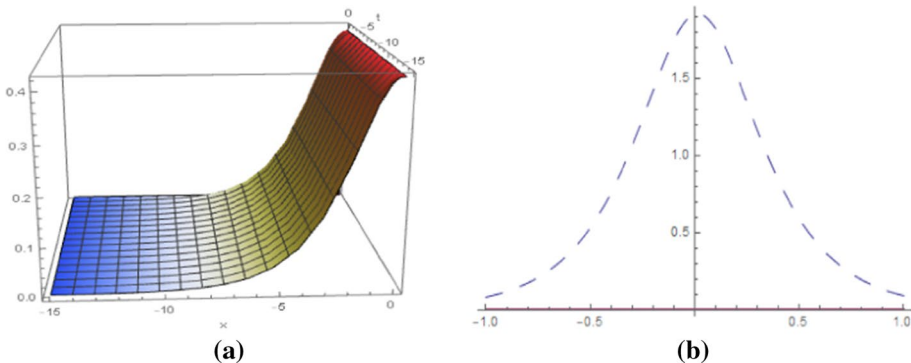


**Fig. 6** The dynamical behavior of the solution  $J_{3,1}(x, t)$  given by Eq. (33) is shown at  $p = 1, T = 5, \gamma = 20, K = 0.7, \omega = 7, r = 15, \alpha = -1, \beta = 3$

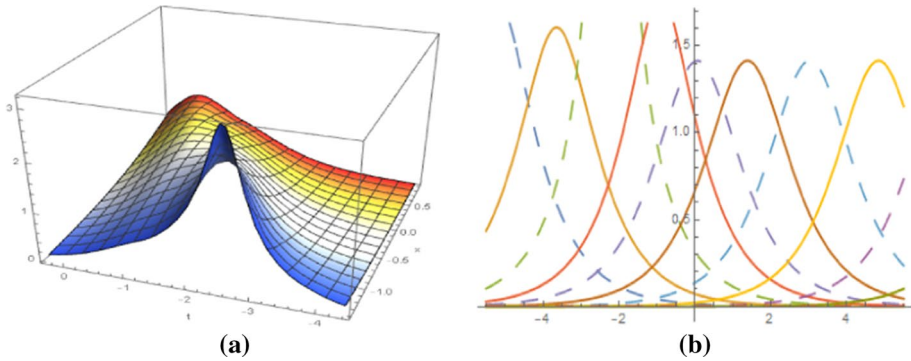


**Fig. 7** The dynamical behavior of the solution  $J_{3,2}(x, t)$  given by Eq. (34) is shown at  $p = 1, T = 5, \gamma = 20, K = 0.7, \omega = 7, r = 15, \alpha = -1, \beta = 3$

$$\mu = \sqrt{\frac{\gamma^2 p^2 \Psi(k^2 - 1)}{2}}; \quad \Lambda = \frac{k^2 + w}{\gamma^2 p^2},$$

provided that

$$J_{3,2}(x, t) = \frac{\sqrt{(-1 + k^2)(-k^2 - 2w)} \operatorname{sech}\left(\eta \sqrt{\frac{k^2 + w}{\gamma}}\right)}{2}. \tag{40}$$

**Type 3c m**  $\rightarrow 1$  By substituting  $\Delta = \Pi = 0$  in Eq. (5) and we get values of following parameters and we obtain the solitary wave solutions (Fig. 8).

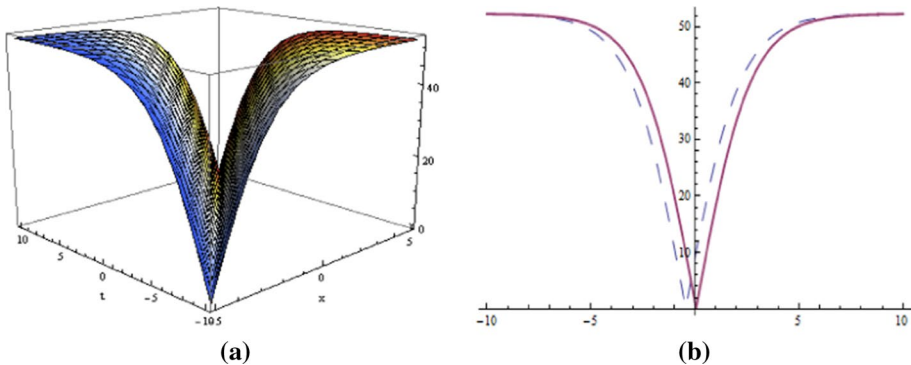


**Fig. 8** The dynamical behavior of the solution  $J_{3,3}(x, t)$  given by Eq. (35) is shown at  $p = 1, T = 5, \gamma = 20, K = 0.7, \omega = 7, r = 15, \alpha = -1, \beta = 3$

$$\mu = \sqrt{\frac{\gamma^2 p^2 \Psi(k^2 - 1)}{2}}; \quad \Lambda = \frac{k^2 + w}{\gamma^2 p^2},$$

provided that

$$J_{3,3}(x, t) = \frac{1}{2} \sqrt{(-1 + k^2)} \sqrt{-(k^2 + 2\omega)} \tanh\left(\frac{\eta \sqrt{\frac{k^2 + 2\omega}{\gamma^2}}}{\sqrt{2}}\right). \tag{41}$$

**Type 6a** By substituting  $\Upsilon = \Delta = \Pi = 0$  in Eq. (5) and we get values of following parameters and we obtained the WEF (Fig. 9).

$$\begin{aligned} \mu &= \sqrt{\frac{\gamma^2 p^2 \Psi(k^2 - 1)}{2}}; \quad \Lambda = \frac{k^2 + w}{\gamma^2 p^2}, \\ J_{6,a}(x, t) &= \frac{\sqrt{(-1 + k^2) p^2 \Psi \gamma^2 - \frac{(k^2 + 2w)}{3p^2 \gamma^2} + \wp\left(p\eta, \frac{4(k^2 + 2w)^2}{3p^4 \gamma^2}, -\frac{8(k^2 + 2w)^3}{27p^6 \gamma^6}\right)}}{\sqrt{2}}. \end{aligned} \tag{42}$$

**Type 6e** By substituting  $\Upsilon = \Delta = \Pi = 0$  in Eq. (5) and we get values of following parameters and we obtain the WEF (Fig. 10).

$$\begin{aligned} \mu &= \sqrt{\frac{\gamma^2 p^2 \Psi(k^2 - 1)}{2}}; \quad \Lambda = \frac{k^2 + w}{\gamma^2 p^2}, \\ J_{6,e}(x, t) &= \frac{3\sqrt{(-1 + k^2) p^2 \Psi \gamma^2} \wp\left(p\eta, \frac{(k^2 + 2w)}{12p^4 \gamma^4}, 0\right)}{\sqrt{2}\left(\frac{k^2 + 2w}{p^2 \gamma^2} + 6\wp\left(p\eta, \frac{(k^2 + 2w)}{12p^4 \gamma^4}, 0\right)\right)}. \end{aligned} \tag{43}$$

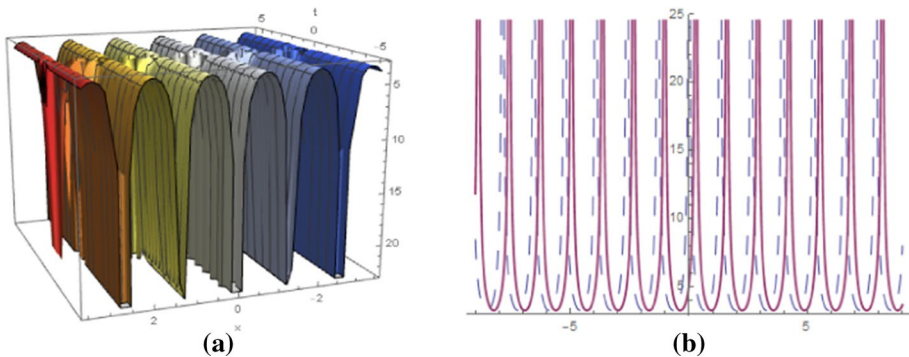


**Fig. 9** The dynamical behavior of the solution  $J_{6,1}(x, t)$  given by Eq. (36) is shown at  $p = 1, T = 5, \gamma = 20, K = 0.7, \omega = 7, r = 15, \alpha = -1, \beta = 3$

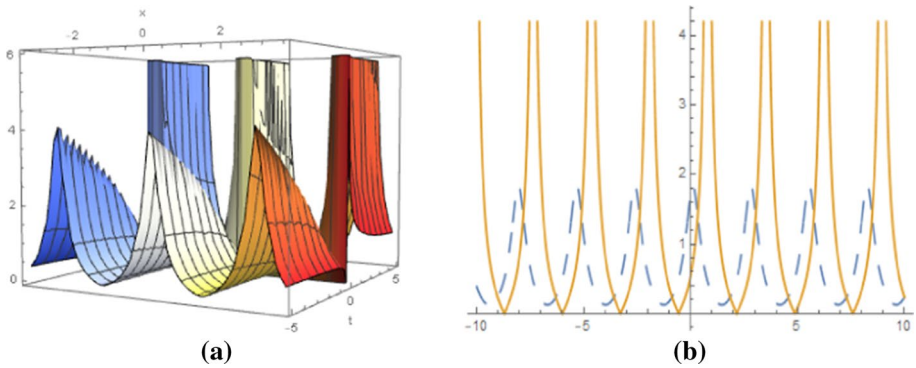


**Fig. 10** The dynamical behavior of the solution  $J_{6,2}(x, t)$  given by Eq. (37) is shown at  $p = 1, T = 5, \gamma = 20, K = 0.7, \omega = 7, r = 15, \alpha = -1, \beta = 3$

**Type 7** By substituting  $\Delta = \Pi = 0, \Upsilon = \frac{5\Lambda^2}{36l}$  in Eq. (5) and we get values of following parameters and we obtained JEF (Fig. 11).

$$\mu = \sqrt{\frac{\gamma^2 p^2 \Psi (k^2 - 1)}{2}}; \quad \Lambda = \frac{k^2 + w}{\gamma^2 p^2},$$

$$J_7(x, t) = \frac{\sqrt{15} \sqrt{(-1 + k^2) p^2 \Psi \gamma^2 (k^2 + 2\omega)} \sqrt{-\frac{k^2 + 2\omega}{p^2 \Psi \gamma^2}} \wp \left( p\eta, \frac{2(k^2 + 2\omega)^2}{9p^4 \gamma^4}, \frac{(k^2 + 2)^3}{54p^6 \gamma^6} \right)}{2(k^2 + 2\omega + 3p^2 \gamma^2 \wp[p\eta, \frac{2(k^2 + 2\omega)^2}{9p^4 \gamma^4}, \frac{(k^2 + 2)^3}{54p^6 \gamma^6}])}. \quad (44)$$

**Type 8a** By substituting  $\Upsilon = \Delta = \Pi = 0$  in Eq. (5) and we get values of following parameters and we obtained the bell type soliton solutions (Fig. 12).

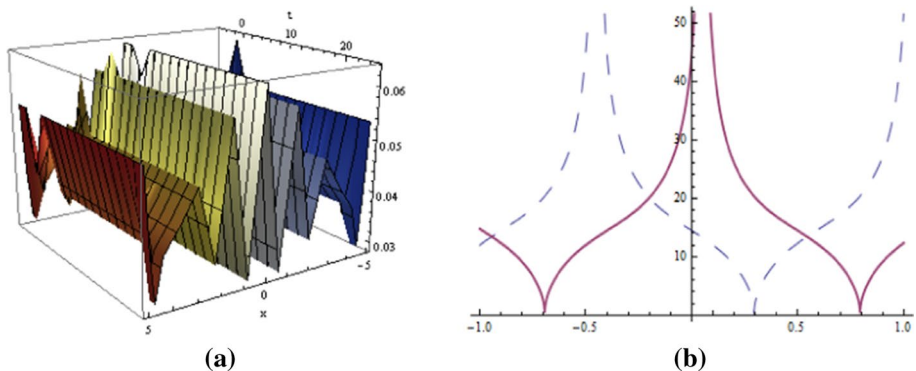


**Fig. 11** The dynamical behavior of the solution  $J_7(x, t)$  given by Eq. (38) is shown at  $p = 1, T = 5, \gamma = 20, K = 0.7, \omega = 7, r = 10, \alpha = -1, \beta = 3$

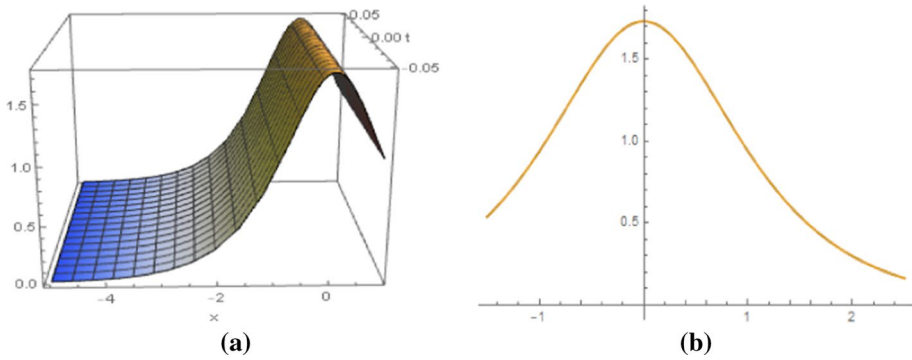


**Fig. 12** The dynamical behavior of the solution  $J_{8,1}(x, t)$  given by Eq. (39) is shown at  $p = 1, T = 5, \gamma = 0.1, K = 0.4, \omega = 0.6, r = 0.1, \alpha = 0.3, \beta = 0.7, \epsilon = 1$

$$\mu = \sqrt{\frac{\gamma^2 p^2 \Psi(k^2 - 1)}{2}}; \quad \Lambda = \frac{k^2 + w}{\gamma^2 p^2},$$

$$J_{8,1}(x, t) = \frac{\sqrt{(-1 + k^2) p^2 \gamma^2} \operatorname{sech}\left(\eta \sqrt{k^2 + 2w}\right)}{\gamma \sqrt{2}}. \tag{45}$$

**Type 8b** By substituting  $\Upsilon = \Delta = \Pi = 0$  in Eq. (5) and we get values of following parameters and we obtain the kink and anti-kink type soliton solutions (Fig. 13).

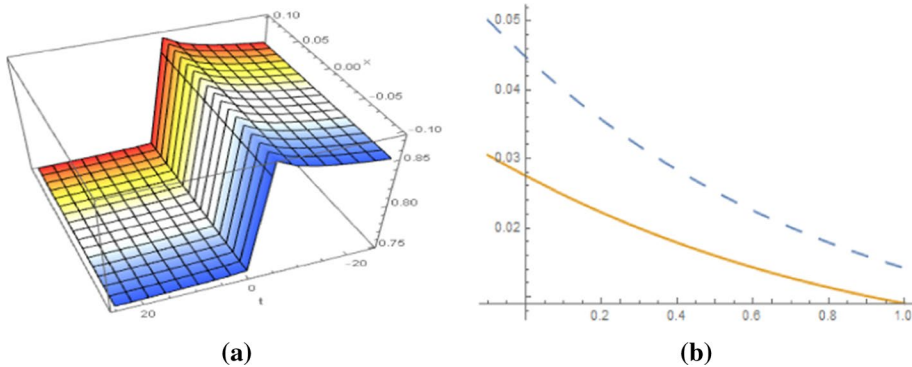


**Fig. 13** The dynamical behavior of the solution  $J_{8,2}(x, t)$  given by Eq. (40) is shown at  $p = 1, T = 5, \gamma = 0.1, K = 0.4, \omega = 0.6, r = 0.1, \alpha = 0.3, \beta = 0.7, \epsilon = 1$

$$\mu = \sqrt{\frac{\gamma^2 p^2 \Psi (k^2 - 1)}{2}}; \quad \Lambda = \frac{k^2 + w}{\gamma^2 p^2},$$

$$J_{8,2}(x, t) = \frac{\sqrt{(-1 + k^2) p^2 \Psi \gamma^2} \sqrt{\frac{k^2 + 2w}{p^2 \gamma^2}} (1 + \epsilon \tanh\left(\frac{1}{2} p \eta \sqrt{\frac{k^2 + 2w}{p^2 \gamma^2}}\right))}{2\sqrt{2}}. \tag{46}$$

**Type 9a** By substituting  $\Upsilon = \Delta = \Pi = 0$  in Eq. (5) and we get values of following parameters and we obtain the bell type soliton solutions (Fig. 14).

$$\mu = \sqrt{\frac{\gamma^2 p^2 \Psi (k^2 - 1)}{2}}; \quad \Lambda = \frac{k^2 + w}{\gamma^2 p^2},$$

$$J_{9,1}(x, t) = \frac{\sqrt{(-1 + k^2) p^2 \Psi \gamma^2} \sqrt{-\frac{\Psi(k^2 + 2w)}{p^2 \gamma^2}} \operatorname{sech}^2\left(\frac{1}{2} p \eta \sqrt{\frac{k^2 + 2w}{p^2 \gamma^2}}\right)}{\sqrt{2} (2\Psi - \Psi \operatorname{sech}^2\left(\frac{1}{2} p \eta \sqrt{\frac{k^2 + 2w}{p^2 \gamma^2}}\right))}. \tag{47}$$

**Type 9b** By substituting  $\Upsilon = \Delta = \Pi = 0$  in Eq. (5) and we get values of following parameters and we obtain the following results (Fig. 15).

$$\mu = \sqrt{\frac{\gamma^2 p^2 \Psi (k^2 - 1)}{2}}; \quad \Lambda = \frac{k^2 + w}{\gamma^2 p^2},$$

$$J_{9,2}(x, t) = -\frac{\sqrt{(-1 + k^2) p^2 \Psi \gamma^2} \sqrt{-\frac{\Psi(k^2 + 2w)}{p^2 \gamma^2}} \operatorname{csch}^2\left(\frac{1}{2} p \eta \sqrt{\frac{k^2 + 2w}{p^2 \gamma^2}}\right)}{\sqrt{2} (2\Psi + \Psi \operatorname{csch}^2\left(\frac{1}{2} p \eta \sqrt{\frac{k^2 + 2w}{p^2 \gamma^2}}\right))}. \tag{48}$$

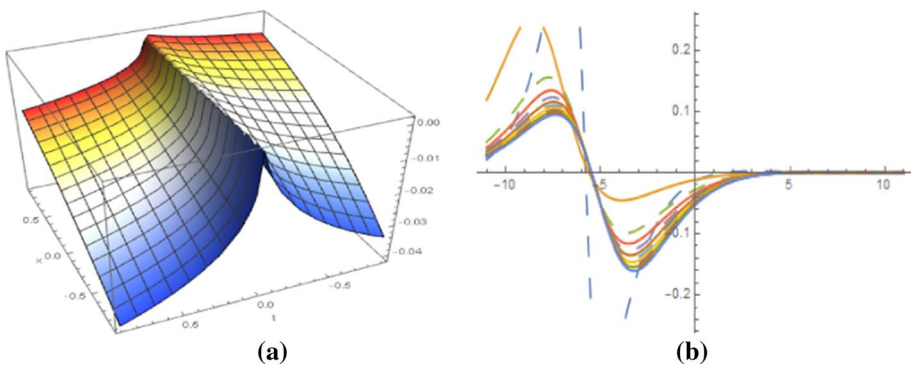


**Fig. 14** The dynamical behavior of the solution  $J_{9,1}(x, t)$  given by Eq. (41) is shown at  $p = 1, T = 5, \gamma = 0.1, K = 0.3, \omega = 0.1, r = 0.1, \alpha = 0.3, \beta = 0.7$

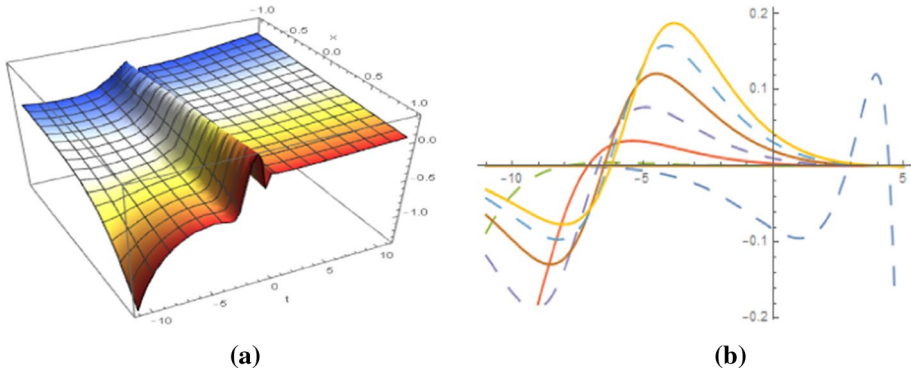


**Fig. 15** The dynamical behavior of the solution  $J_{9,2}(x,t)$  given by Eq. (42) is at  $p = 1, T = 5, \gamma = 0.1, K = 0.3, \omega = 0.1, r = 0.1, \alpha = 0.3, \beta = 0.7$

**Type 10a** By substituting  $\Upsilon = \Delta = \Pi = 0$  in Eq. (5) and we get values of following parameters and we obtain the bell type soliton solutions (Fig. 16).

$$\mu = \sqrt{\frac{\gamma^2 p^2 \Psi(k^2 - 1)}{2}}; \quad \Lambda = \frac{k^2 + w}{\gamma^2 p^2},$$

$$J_{10,1}(x,t) = - \frac{\sqrt{(-1 + k^2) p^2 \Psi \gamma^2} \sqrt{-\frac{\Psi(k^2 + 2w)}{p^2 \gamma^2}} \sec^2 \left( \frac{1}{2} p \eta \sqrt{-\frac{k^2 + 2w}{p^2 \gamma^2}} \right)}{\sqrt{2} \Psi \left( -2 - \sec^2 \left( \frac{1}{2} p \eta \sqrt{-\frac{k^2 + 2w}{p^2 \gamma^2}} \right) \right)} \quad (49)$$

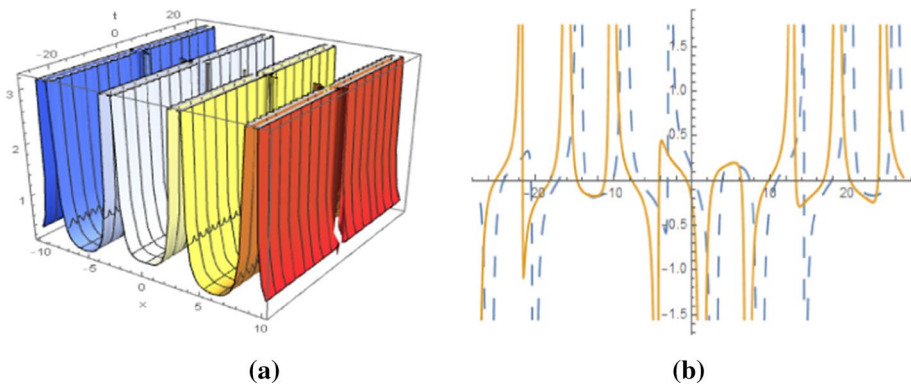


**Fig. 16** The dynamical behavior of the solution  $J_{10,1}(x,t)$  given by Eq. (43) is at  $p = 1, T = 5, \gamma = 10, K = 0.9, \omega = -1, r = 1, \alpha = -1, \beta = 0.1$

**Type 10b** By substituting  $\Upsilon = \Delta = \Pi = 0$  in Eq. (5) and we get values of following parameters and we obtain the solitary wave solutions (Fig. 17).

$$\mu = \sqrt{\frac{\gamma^2 p^2 \Psi(k^2 - 1)}{2}}; \quad \Lambda = \frac{k^2 + w}{\gamma^2 p^2},$$

$$J_{10,2}(x, t) = - \frac{\sqrt{(-1 + k^2) p^2 \Psi \gamma^2} \sqrt{-\frac{\Psi(k^2+2w)}{p^2 \gamma^2}} \operatorname{csc}^2 \left( \frac{1}{2} p \eta \sqrt{-\frac{k^2+2w}{p^2 \gamma^2}} \right)}{\sqrt{2} \Psi \left( -2 + \operatorname{csc}^2 \left( \frac{1}{2} p \eta \sqrt{-\frac{k^2+2w}{p^2 \gamma^2}} \right) \right)}. \quad (50)$$

### 4 Sub-ODE method

By applying transformation in Eq. (3),  $\zeta = k(x - \omega t)$ , here  $k > 0$ , we get

$$(A\omega)U_\zeta + k^2 U_{\zeta\zeta\zeta} + Ak\omega U^2 = 0, \quad (51)$$

let  $U_\zeta = V$ , it will give us

$$(A\omega)V + k^2 \omega V'' + Ak\omega V^2 = 0, \quad (52)$$

By balancing technique we get  $2p = m$ .

By putting Eq. (48) into Eq. (5), we get the following set of algebraic equations:

$$G^{4p}(\eta) : 6k^2 p^2 T \mu \omega + Ak \mu^2 \omega = 0, \quad (53)$$

$$G^{2p}(\eta) : A\mu - \mu \omega + 4Ck^2 p^2 \mu \omega = 0, \quad (54)$$

we have the following types of solutions:

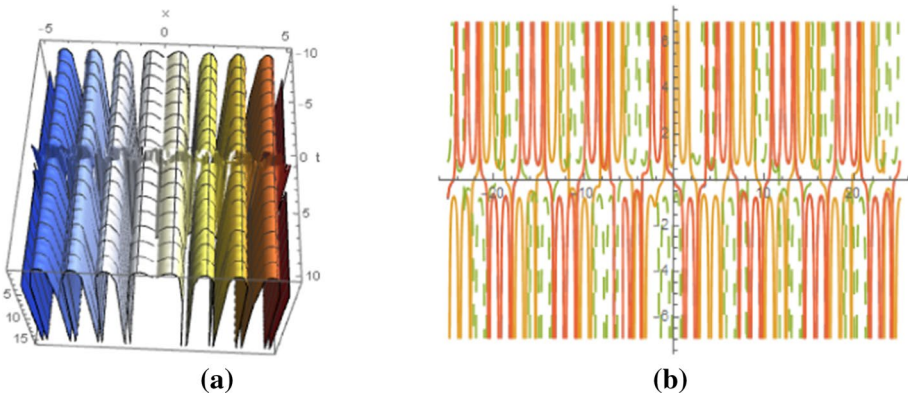


**Fig. 17** The dynamical behavior of the solution  $J_{10,2}(x, t)$  given by Eq. (44) is shown at  $p = 1, T = 5, \gamma = 10, K = 0.9, \omega = -1, r = 1, \alpha = -1, \beta = 0.1$



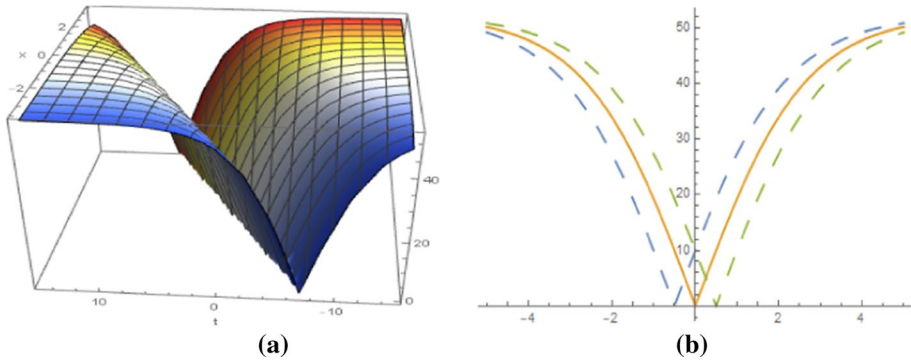


**Fig. 18** The dynamical behavior of the solution  $\Theta_{2,1}(x,t)$  given by Eq. (51) is shown at  $p = 1, T = 5, \gamma = 20, K = 0.7, \omega = 7, r = 10, \alpha = -1, \beta = 3, \epsilon = 1$

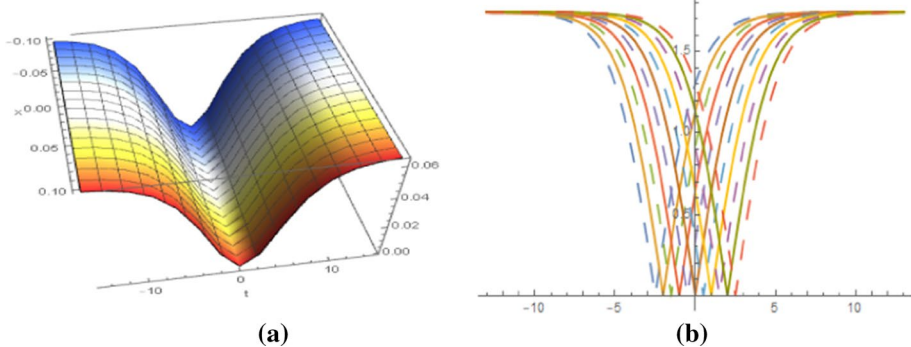


**Fig. 19** The dynamical behavior of the solution  $\Theta_{2,2}(x,t)$  given by Eq. (52) is shown at  $p = 1, T = 5, \gamma = 20, K = 0.7, \omega = 7, r = 10, \alpha = -1, \beta = 3, \epsilon = 1$

**Type 2a** By substituting  $Y = \Delta = \Pi = 0$  in Eq. (5) and we get values of following parameters and we obtain the kink and anti-kink type soliton solutions (Fig. 18).

$$\mu = -\frac{6kp^2T}{A}; \Lambda = \frac{-A + \omega}{4\omega k^2 p^2 \omega},$$

$$\Theta_{2,1}(x, t) = \frac{3\epsilon^2(-A + \omega) \tanh\left(\frac{p\xi\sqrt{1+\frac{A}{\omega}}}{2kp}\right)^2}{2Ak\omega}. \tag{55}$$

**Type 2b** By substituting  $Y = \Delta = \Pi = 0$  in Eq. (5) and we get values of following parameters and we obtain the kink and anti-kink type soliton solutions (Fig. 19).

$$\begin{aligned} \mu &= -\frac{6kp^2T}{A}; & \Lambda &= \frac{-A + \omega}{4\omega k^2 p^2 \omega}, \\ \Theta_{2,2}(x, t) &= \frac{3\epsilon^2(-A + \omega) \tan\left(\frac{p\xi\sqrt{1+\frac{t}{\omega}}}{2kp}\right)^2}{2Ak\omega}. \end{aligned} \tag{56}$$

**Type 3a** ( $m \rightarrow 1$ ) By substituting  $\Upsilon = \Delta = \Pi = 0$  in Eq. (5) and we get values of following parameters and we obtain periodic solutions (Fig. 20).

$$\begin{aligned} \mu &= -\frac{6kp^2T}{A}; & \Lambda &= \frac{-A + \omega}{4\omega k^2 p^2 \omega}, \\ \Theta_{3,1}(x, t) &= \frac{-3A + 3\omega}{Ak\omega + Ak\omega \cosh\left(\frac{p\xi\sqrt{\frac{-A+\omega}{\omega}}}{kp}\right)}. \end{aligned} \tag{57}$$

**Type 3b** ( $m \rightarrow 1$ ) By substituting  $\Upsilon = \Delta = \Pi = 0$  in Eq. (5) and we get values of following parameters and we obtain the periodic solutions (Fig. 21).

$$\begin{aligned} \mu &= -\frac{6kp^2T}{A}; & \Lambda &= \frac{-A + \omega}{4\omega k^2 p^2 \omega}, \\ \Theta_{3,1}(x, t) &= \frac{-3A + 3\omega}{2Ak\omega + 2Ak\omega \cosh\left(\frac{p\xi\sqrt{\frac{-A+\omega}{\omega}}}{\sqrt{2}kp}\right)}. \end{aligned} \tag{58}$$

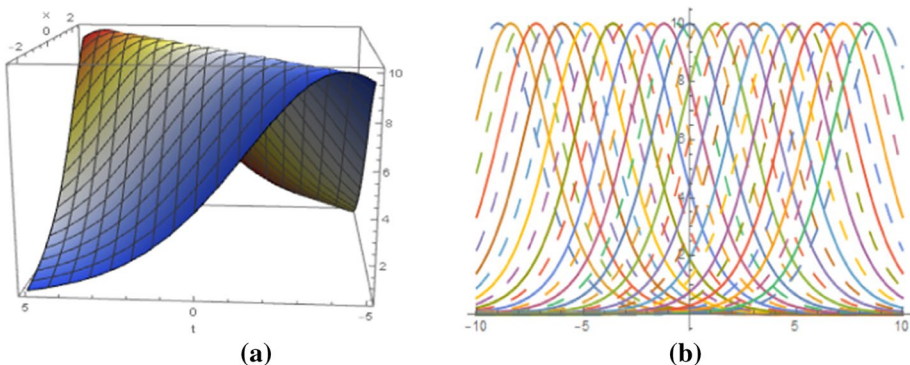


**Fig. 20** The dynamical behavior of the solution  $\Theta_{3,1}(x, t)$  given by Eq. (53) is shown at  $p = 1, T = 5, \gamma = 20, K = 0.7, \omega = 7, r = 10, \alpha = -1, \beta = 3, \epsilon = 1$

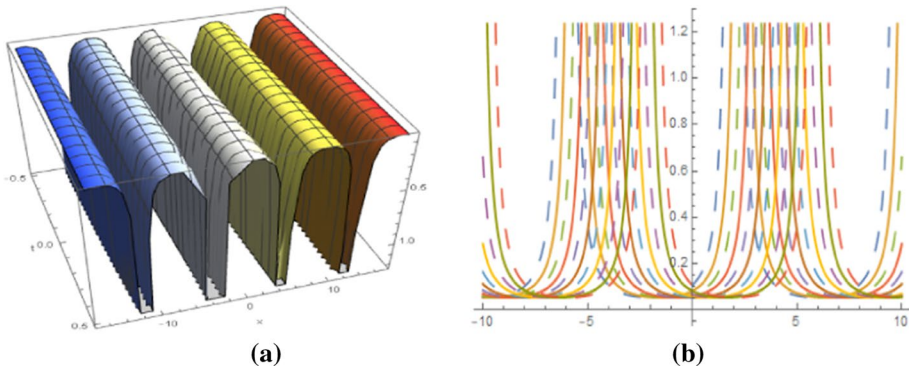


**Fig. 21** The dynamical behavior of the solution  $\Theta_{3,2}(x,t)$  given by Eq. (54) is shown at  $p = 1, T = 5, \gamma = 20, K = 0.7, \omega = 7, r = 10, \alpha = -1, \beta = 3, \epsilon = 1$

**Type 3c** ( $m \rightarrow 1$ ) By substituting  $\Upsilon = \Delta = \Pi = 0$  in Eq. (5) and we get values of following parameters and we obtain the kink and anti-kink type soliton solutions (Fig. 22).

$$\mu = -\frac{6kp^2T}{A}; \quad \Lambda = \frac{-A + \omega}{4\omega k^2 p^2 \omega},$$

$$\Theta_{3,3}(x,t) = \frac{3(-A + \omega) \tanh\left(\frac{p\xi \sqrt{-1 + \frac{A}{\omega}}}{2\sqrt{2}kp}\right)^2}{4Ak\omega}. \tag{59}$$

**Type 6a** By substituting  $\Upsilon = \Delta = \Pi = 0$  in Eq. (5) and we get values of following parameters and we obtain the WEF (Fig. 23).

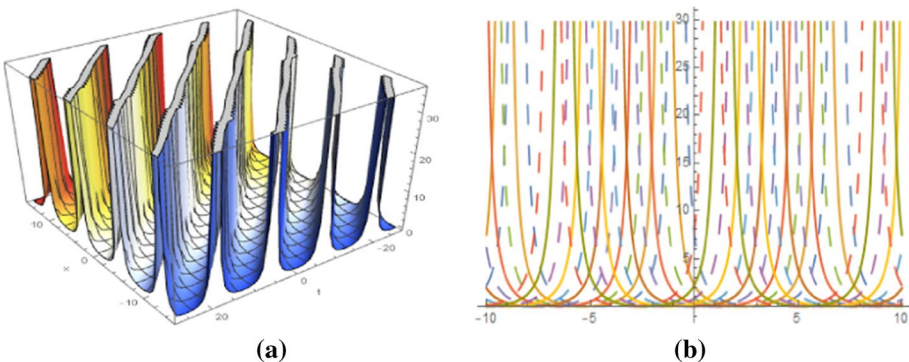


**Fig. 22** The dynamical behavior of the solution  $\Theta_{3,3}(x,t)$  given by Eq. (55) is shown at  $p = 1, T = 5, \gamma = 20, K = 0.7, \omega = 7, r = 10, \alpha = -1, \beta = 3, \epsilon = 1$

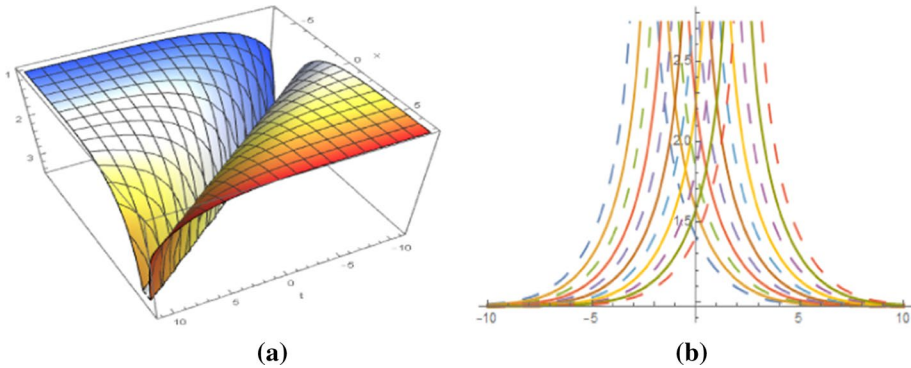


**Fig. 23** The dynamical behavior of the solution  $\Theta_{6,1}(x, t)$  given by Eq. (56) is shown at  $p = 1, T = 5, \gamma = 20, K = 0.7, \omega = 7, r = 10, \alpha = -1, \beta = 3, \epsilon = 1$

$$\mu = -\frac{6kp^2T}{A}; \quad \Lambda = \frac{-A + \omega}{4\omega k^2 p^2 \omega},$$

$$\Theta_{6,1}(x, t) = -\frac{6kp^2T \left( \frac{A-\omega}{12k^2 p^2 \omega} + \frac{\wp \left( p\xi, \frac{1}{3} \left( -12AT + \frac{(A-\omega)^2}{4k^4 p^4 \omega^2} \right), \frac{(A-\omega)(A^2 - 2A\omega + (1-72ATk^4 p^4)\omega^2)}{216k^6 p^6 \omega^3} \right)}{T} \right)^{\frac{1}{4}}}{A} \quad (60)$$

**Type 6e** By substituting  $Y = \Delta = \Pi = 0$  in Eq. (5) and we get values of following parameters and we obtain the WEF (Fig. 24).

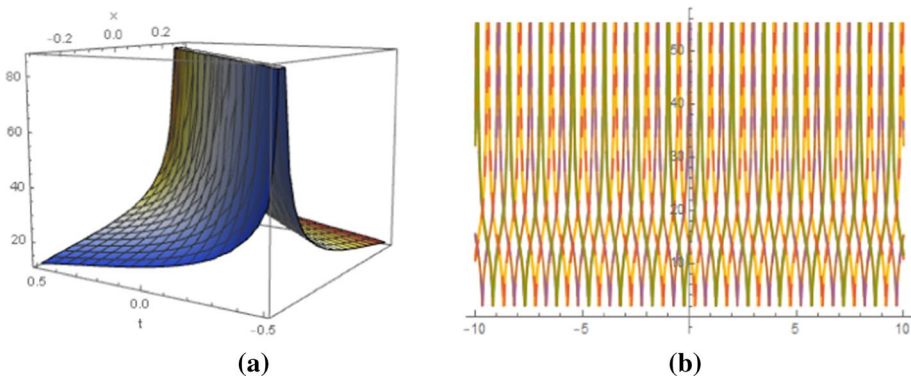


**Fig. 24** The dynamical behavior of the solution  $\Theta_{6,2}(x, t)$  given by Eq. (57) is shown at  $p = 1, T = 5, \gamma = 20, K = 0.7, \omega = 7, r = 10, \alpha = -1, \beta = 3, \epsilon = 1$

$$\mu = -\frac{6kp^2T}{A}; \quad \Lambda = \frac{-A + \omega}{4\omega k^2 p^2 \omega},$$

$$\Theta_{6,2}(x, t) = -\frac{12 \sqrt{3kp^2T} \sqrt{\frac{k^2 p^2 \sqrt{\frac{1}{T}} \wp_{\text{prime}}\left(P\xi, AT + \frac{(A-\omega)^2}{192k^4 p^4 \omega^2}, \frac{AT\xi^3}{6}\right)}{-A + \omega + 24k^2 p^2 \omega \wp\left(P\xi, AT + \frac{(A-\omega)^2}{192k^4 p^4 \omega^2}, \frac{AT\xi^3}{6}\right)}}{A} \tag{61}$$

**Type 7** By substituting  $\Delta = \Pi = 0$ ,  $\Upsilon = \frac{5\Lambda^2}{36T}$  in Eq. (5) and we get values of following parameters and we obtained the WEF (Fig. 25).

$$\mu = -\frac{6kp^2T}{A}; \quad \Lambda = \frac{-A + \omega}{4\omega k^2 p^2 \omega},$$

$$\Theta_7(x, t) = -\frac{45(A - \omega)^3 \wp\left(p\xi, \frac{(A+\omega)^2}{72k^4 p^4 \omega^2}, \frac{(-A+\omega)^3}{3456k^6 p^6 \omega^3}\right)^2}{4Ak\omega(-A + \omega + 12k^2 p^2 \omega \wp\left(p\xi, \frac{(A+\omega)^2}{72k^4 p^4 \omega^2}, \frac{(-A+\omega)^3}{3456k^6 p^6 \omega^3}\right))^2} \tag{62}$$

### 5 Results and discussion with graphical description

In this article, we have examined Atangana–Baleanu (AB) fractional system of equations for the ion sound and Langmuir waves (ISALWs) and HRE to gain different solitons. Under different conditions, we apply Sub-ODE procedure to both above models and perceived effective results. Tripathya and Sahoo (2020) derived exact solutions for ISLAWs equation. Baskonus and Bulut (2016) studied different modes of ISLAWs equations. Seadawy

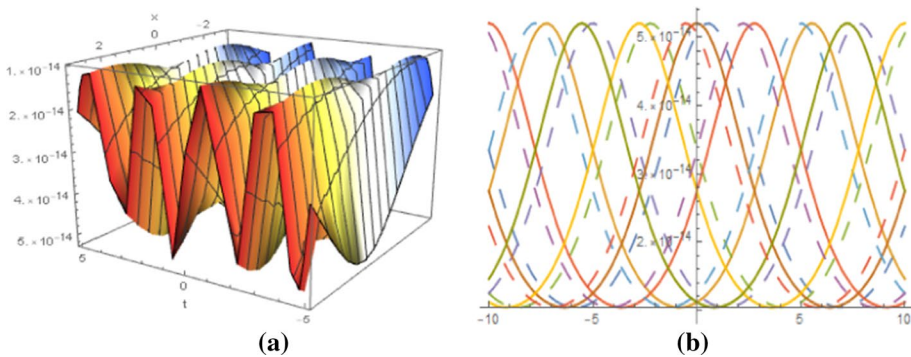


**Fig. 25** The dynamical behavior of the solution  $\Theta_{7,1}(x, t)$  given by Eq. (58) is shown at  $p = 1, T = 5, \gamma = 20, K = 0.7, \omega = 7, r = 10, \alpha = -1, \beta = 3, \epsilon = 1$

et al. (2019a) discussed about structure of ISLAWs equation and also its applications. Ahmed et al. (2019a) generate Rogue waves and studied about relationship of multi-peak solitons for the system of equations of ISLAWs. Koonprasert and Punpocha (2016) applied F-Expansion method on Hirota–Ramani equation. Qi et al. (2004) acquired traveling solutions to Hirota equation. Zhao and Tam (2006) find soliton solutions for a coupled Ramani equation. We derived out bright, dark, singular and periodic wave solution for ISLAWs equation. We also retrieved bell type, kink type, periodic, rational, (JEF) and (WEF) solutions for Ramani equation. The bell type solution are shown by Eqs. (8), (21) and (58) while the kink type is represented by Eqs. (10) and (19). Some periodic solutions have also been derived and are given by Eqs. (8), (11), (23) and (24). A rational solution is also discussed in Eq. (9). Some JEF are found from Eqs. (12)–(14) along with the conditions mentioned therein. whereas the WEF are represented by Eqs. (15)–(17). In addition to these, some more solutions have also been given in Eq. (22) singular soliton. A graphical description of these results has also been given.

## 6 Conclusion

We describe exact solution of NLFEE above we study the graphical representation of various types of solutions. We obtained the different solutions of model name which consists of dark soliton, bright soliton, Jacobi elliptic solutions (JES), Weierstrass elliptic solitons (WES), hyperbolic solutions and parabolic solutions. For better understanding we express 3D, 2D and contour view. We claim that the achieved solutions are distinct and very helpful for the study of model name.

**Funding** Not applicable.

**Data availability** Not applicable.

## Declarations

**Conflicts of interest** The authors declare no conflict of interest.

**Ethical approval** I hereby declare that this manuscript is the result of my independent creation under the reviewers' comments. Except for the quoted contents, this manuscript does not contain any research achievements that have been published or written by other individuals or groups.

## References

- Abazari, R., Jamshidzadeh, S., Biswas, A.: Solitary Wave Solutions of Coupled Boussinesq Equation. Wiley Periodicals Inc., Hoboken (2016)
- Ahmad, S., Ashraf, R., Seadawy, A.R., Rizvi, S.T.R., Younis, M., Althobaiti, A., El-Shehawi, A.M.: Lump, multiwave, kinky breathers, interactional solutions and stability analysis for (2+1)-rth dispersionless Dym equation. *Results Phys.* **25**, 104160 (2021)
- Ahmed, I., Seadawy, A.R., Lu, D.: Rogue waves generation and interaction of multi-peak rational solitons in the system of equations for the ion sound and Langmuir waves. *Int. J. Mod. Phys. B* **33**, 1–9 (2019a)
- Ahmed, I., Seadawy, A.R., Dianchen, L.: Kinky breathers, W-shaped and multi-peak solitons interaction in (2+1)-dimensional nonlinear Schrödinger's equation with Kerr law of nonlinearity. *Eur. Phys. J. Plus* **134**(120), 1–11 (2019b)



- Akram, U., Seadawy, A.R., Rizvi, S.T.R., Younis, M., Althobaiti, S., Sayed, S.: Traveling waves solutions for the fractional Wazwaz Benjamin Bona Mahony model in arising shallow water waves. *Results Phys.* **20**, 103725 (2021)
- Atangana, A., Gómez-Aguila, J.F.: Numerical approximation of Riemann–Liouville definition of fractional derivative: from Riemann–Liouville to Atangana–Baleanu. *Numer. Methods Partial Differ. Equ.* **34**, 1502–1523 (2018)
- Atangana, A., Baleanu, D.: New fractional derivatives with nonlocal and non-singular kernel: theory and application to heat transfer model. *Therm. Sci.* **20**, 763–769 (2016)
- Atangana, A., Koca, I.: Chaos in a simple nonlinear system with Atangana–Baleanu derivatives with fractional order. *Journals and Books* **89**, 447–454 (2016)
- Baleanu, D., Jajarmi, A., Hajipour, M.: On the nonlinear dynamical systems within the generalized fractional derivatives with Mittag–Leffler kernel. *Nonlinear Dyn.* **94**, 397–414 (2018)
- Bas, E., Ozarslan, R.: Real world applications of fractional models by Atangana–Baleanu fractional derivative. *Chaos Solitons Fract* **116**, 121–125 (2018)
- Bashir, A., Seadawy, A.R., Rizvi, S.T.R., Younis, M., Ali, I., Mousa, A.A.A.: Application of scaling invariance approach, P-test and soliton solutions for couple of dynamical models. *Results Phys.* **25**, 104227 (2021)
- Baskonus, H.M., Bulut, H.: New wave behaviors of the system of equations for the ion sound and Langmuir Waves. *Waves Random Complex Media* **26**, 613–625 (2016)
- Bilal, M., Seadawy, A.R., Younis, M., Rizvi, S.T.R., Rashidy, A.E., Mahmoud, S.F.M.: Analytical wave structures in plasma Physics modeled by Gilson Pickering equation by two integration norms. *Results Phys.* **23**, 103959 (2021)
- Dianchen, L., Seadawy, A., Arshad, M.: Bright–Dark optical soliton and dispersive elliptic function solutions of unstable nonlinear Schrodinger equation and its applications. *Opt. Quantum Electron.* **50**(23), 1–10 (2018)
- Fernandez, A., Baleanu, D., Srivastava, H.M.: Series representations for fractional-calculus operators involving generalised Mittag–Leffler functions. *Commun. Nonlinear Sci* **67**, 517–527 (2019)
- Ghanbari, B., Atangana, A.: A new application of fractional Atangana–Baleanu derivatives: designing ABC-fractional masks in image processing. *Phys. A* **542**, 123516 (2020)
- Ghanbari, B., Yusuf, A., Baleanu, D.: The new exact solitary wave solutions and stability analysis for the (2+1)-dimensional Zakharov–Kuznetsov equation. *Adv. Differ. Equ.* (2019). <https://doi.org/10.1186/s13662-019-1964-0>
- Jarada, F., Abdeljawad, T., Hammouch, Z.: On a class of ordinary differential equations in the frame of Atangana–Baleanu fractional derivative. *Chaos, Solitons Fractals* **117**, 16–20 (2018)
- Khater, A.H., Callebaut, D.K., Seadawy, A.R.: General soliton solutions for nonlinear dispersive waves in convective type instabilities. *Phys. Scr.* **74**, 384–393 (2006)
- Koonprasert, S., Punpocha, M.: More exact solutions of Hirota–Ramani partial differential equations by applying F-expansion method and symbolic computation. *Glob. J. Pure Appl. Math.* **12**, 1903–1920 (2016)
- Kurt, A.: New periodic wave solutions of a time fractional integrable shallow water equation. *Appl. Ocean Res.* **85**, 128–135 (2019)
- Owolabi, K.M.: Modelling and simulation of a dynamical system with the Atangana–Baleanu fractional derivative. *Eur. Phys. J. plus* **133**, 15 (2018)
- Peter, O.J., Shaikh, A.S., Ibrahim, M.O., Nisar, K.S., Baleanu, D., Khan, I., Abioye1, A.I.: Analysis and Dynamics of Fractional Order Mathematical Model of COVID-19 in Nigeria Using Atangana–Baleanu Operator, *Tech Science Press*, 26, 02 (2021)
- Qi, W., Yong, C., Biao, L., Qing, Z.H.: New exact travelling wave solutions to Hirota equation and (1+1)-dimensional dispersive long wave equation. *Commun. Theor. Phys.* **41**, 821 (2004)
- Rezazadeh, H., Adel, W., Tebue, E.T., Yao, S.W., Inc, M.: Bright and singular soliton solutions to the Atangana–Baleanu fractional system of equations for the ISALWs. *J. King Saud Univ.* **33**, 101420 (2021)
- Rizvi, S.T.R., Ali, K., Ahmad, M.: Optical solitons for Biswas–Milovic equation by new extended auxiliary equation method. *Optik* **204**, 164181 (2020a)
- Rizvi, S.T.R., Afzal, I., Ali, K.: Dark and singular optical solitons for Kundu–Mukherjee–Naskar model. *Mod. Phys. Lett. B* **34**, 9 (2020b)
- Rizvi, S.T.R., Ali, I., Seadawy, A.R., Younis, M., Bibi, I.: Chirp-free optical dromions for the presence of higher order spatio-temporal dispersions and absence of self-phase modulation in birefringent fibers. *Mod. Phys. Lett. B* **34**, 2050399 (2020c)
- Rizvi, S.T.R., Seadawy, A.R., Bibi, I., Younis, M.: Chirped and chirp-free optical solitons for Heisenberg ferromagnetic spin chains model. *Mod. Phys. Lett. B* **35**, 2150139 (2021a)

- Rizvi, S.T.R., Seadawy, A.R., Younis, M., Ali, I., Althobaiti, S., Mahmoud, S.F.: Soliton solutions, Painleve analysis and conservation laws for a nonlinear evolution equation. *Results Phys.* **23**, 103999 (2021b)
- Rizvi, S.T.R., Seadawy, A.R., Younis, M., Iqbal, S., Althobaiti, S., El-Shehawi, A.M.: Various optical dromions for a weak fractional NLSE with parabolic law. *Results Phys.* **23**, 103998 (2021c)
- Roshid, H.O., Alam, M.N.: Multi-soliton solutions to nonlinear Hirota–Ramani equation. *Appl. Math. Inf. Sci* **11**, 723–727 (2017)
- Seadawy, A.R., Ali, A., Lu, D.: Structure of system solutions of ion sound and Langmuir dynamical models and their applications. *Pramana J. Phys.* **92**, 1–14 (2019a)
- Seadawy, A.R., Ali, A., Albarakati, W.A.: Analytical wave solutions of the  $(2 + 1)$ -dimensional first integro-differential Kadomtsev–Petviashvili hierarchy equation by using modified mathematical methods. *Results Phys.* **15**, 102775 (2019b)
- Seadawy, A.R., Iqbal, M., Lu, D.: Application of mathematical methods on the ion sound and Langmuir waves dynamical systems. *Pramana J. Phys.* **93**, 10 (2019c). <https://doi.org/10.1007/s12043-019-1771-x>
- Seadawy, A.R., Rizvi, S.T.R., Ali, I., Younis, M., Ali, K., Makhlof, M.M., Althobaiti, A.: Conservation laws, optical molecules, modulation instability and Painleve analysis for Chen–Lee–Liu model. *Opt. Quant. Electron.* **53**, 172 (2021a)
- Seadawy, A.R., Bilal, M., Younis, M., Rizvi, S.T.R., Makhlof, M.M., Althobaiti, S.: Optical solitons to birefringent fibers for coupled RKL model without four wave mixing. *Opt. Quant. Electron.* **53**, 324 (2021b)
- Seadawy, A.R., Bilal, M., Younis, M., Rizvi, S.T.R., Althobaiti, S., Makhlof, M.M.: Analytical mathematical approaches for the double chain model of DNA by a novel computational technique. *Chaos Solitons Fract.* **144**, 110669 (2021c)
- Seadawy, A.R., Rehman, S.U., Younis, M., Rizvi, S.T.R., Althobaiti, S., Makhlof, M.M.: Modulation Instability analysis and longitudinal wave propagation in an elastic cylindrical rod modeled with Pochhammer–Chree equation and its modulation instability analysis. *Phys. Scr.* **96**(4), 045202 (2021d)
- Seadawy, A.R., Rizvi, S.T.R., Ahmad, S., Younis, M., Baleanu, D.: Lump, lump one stripe, multiwaves and breather solutions for the Hunter Sexton equation. *Open Phys.* **19**, 1–20 (2021e)
- Sheng, J., Jiang, W., Pang, D.: Finite-time stability of Atangana–Baleanu fractional-order linear systems. *Complexity* (2020). <https://doi.org/10.1155/2020/1727358>
- Syama, M.I., Al-Refai, M.: Fractional differential equations with Atangana–Baleanu fractional derivative: Analysis and applications. *Chaos, Solitons and Fractals: X* **2**, 100013 (2019)
- Tariq, K.U., Zainab, H., Seadawy, A.R., Younis, M., Rizvi, S.T.R.: On some traveling wave solutions to the paraxial M-fractional nonlinear Schrödinger equation. *Opt. Quant. Electron.* **53**, 219 (2021)
- Tripathya, A., Sahoo, S.: Exact solutions for the ion sound Langmuir wave model by using two novel analytical methods. *Results Phys.* **19**, 103494 (2020)
- Younas, U., Younis, M., Seadawy, A.R., Rizvi, S.T.R., Althobaiti, S., Sayed, S.: Diverse exact solutions for modified nonlinear Schrödinger equation with conformable fractional derivative. *Results Phys.* **20**, 103766 (2021)
- Zayeda, E.M.E., Shohiba, R.M.A., Biswas, A., Yıldırım, Y., Mallawic, F., Belic, M.R.: Chirped and chirp-free solitons in optical fiber Bragg gratings with dispersive reflectivity having parabolic law nonlinearity by Jacobi's elliptic function. *Results Phys.* **15**, 102784 (2019)
- Zhao, J.X., Tam, H.W.: Soliton solutions of a coupled Ramani equation. *Appl. Math. Lett.* **19**, 307–313 (2006)

**Publisher's Note** Springer Nature remains neutral with regard to jurisdictional claims in published maps and institutional affiliations.

Springer Nature or its licensor holds exclusive rights to this article under a publishing agreement with the author(s) or other rightsholder(s); author self-archiving of the accepted manuscript version of this article is solely governed by the terms of such publishing agreement and applicable law.